Fluid Dynamics, Vol. 41, No. 1, 2006, pp. 37–48. Translated from Izvestiya Rossiiskoi Academii Nauk, Mekhanika Zhidkosti i Gaza, No. 1, 2006, pp. 42–53.

Numerical Modeling of the Receptivity of a Supersonic Boundary Layer to Acoustic Disturbances

I. V. Egorov, V. G. Sudakov, and A. V. Fedorov

Received February 4, 2005

Abstract — The receptivity of a supersonic ($M_\infty = 6$) boundary layer on a flat plate to acoustic disturbances is investigated on the basis of a numerical solution of the 2D Navier-Stokes equations. Numerical results obtained for fast and slow acoustic waves impinging on the plate at zero angle agree qualitatively with asymptotic theory. Calculations carried out for other angles of incidence of the acoustic waves reveal new features of the perturbation field in the neighborhood of the leading edge of the plate. It is shown that, due to visco-inviscid interaction, the shock formed near the leading edge may significantly affect the acoustic field and the receptivity.

Keywords: Navier-Stokes equations, supersonic flow, boundary layer, perturbations, numerical modeling, acoustics.

The prediction of laminar-turbulent transition is an important problem for high-speed vehicle design and drag calculations [1]. A review of the advances made in the methods of calculating the transition Reynolds number can be found in [2]. Experimental studies in hypersonic wind tunnels are very limited. Direct numerical simulation can fill this gap because numerical experiment provides detailed information about the perturbation field. This method can be used for developing and verifying theoretical models and also for modeling complex flows, to which the methods of stability theory, such as the use of parabolized stability equations, are not applicable. This explains the growing interest in direct numerical modeling of the laminar-turbulent transition. In particular, the receptivity and stability have been modeled numerically for a hypersonic boundary layer on a parabolic leading edge [3] and on a flat plate [4, 5].

A theoretical model of the receptivity of a supersonic boundary layer on a flat plate with respect to acoustic perturbations was developed in [6, 7]. This model describes the physics of local receptivity related with diffraction and scattering of acoustic waves near the leading edge of the plate. In [8], the theoretical results are compared with wind-tunnel experimental data [9, 10].

In this study, using a second-order TVD scheme [11], we solve the Navier Stokes equations for 2D unsteady, compressible flows. This makes it possible to model fairly accurately the scattering and diffraction of acoustic disturbances near the leading edge of the plate. An investigation of the growth of the perturbations induced by local periodic injection-suction in a supersonic boundary layer showed that the calculation method used is valid for the problems of receptivity and stability of a supersonic boundary layer [11].

In the present study, we numerically model the receptivity of the boundary layer on a flat plate ($M_\infty = 6$) with respect to acoustic disturbances. The numerical results obtained for fast and slow acoustic waves incident at zero angle are compared with the theoretical data of [6, 7] and numerical modeling [5]. Numerical experiments performed for angles of incidence of the acoustic disturbances equal to $\pm 45^\circ$ reveal new features of the perturbation field near the leading edge, which can play an important role in the receptivity process.

1. FORMULATION OF THE PROBLEM AND NUMERICAL METHOD

Viscous compressible flows are described by the Navier-Stokes equations following from the mass, momentum, and energy balance laws. For 2D unsteady flows, the Navier-Stokes equations are written in

0015–4628/06/4101–0037

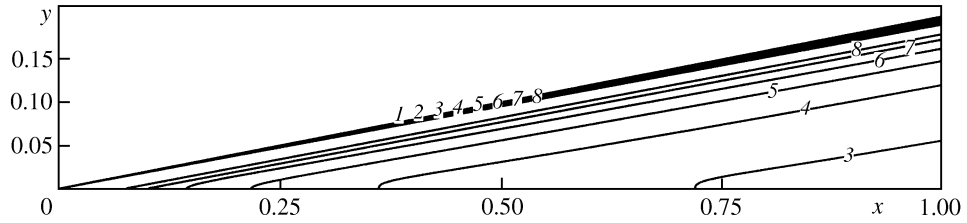

Fig. 1. Steady-state pressure field for $M_\infty = 6$, $Re_\infty = 2 \cdot 10^6$; $p = 0.0200$ (curve *1*), 0.0204 (*2*), 0.0208 (*3*), 0.0212 (*4*), 0.0216 (*5*), 0.0220 (*6*), 0.0224 (*7*), 0.0228 (*8*)

nondimensional conservative form in the curvilinear coordinates (ξ, η) (where $x = x(\xi, \eta)$ and $y = y(\xi, \eta)$ are Cartesian coordinates):

$$\frac{\partial \mathbf{Q}}{\partial t} + \frac{\partial \mathbf{E}}{\partial \xi} + \frac{\partial \mathbf{G}}{\partial \eta} = 0$$

Here, $\mathbf{Q}$ is the vector of the conservative dependent variables, and $\mathbf{E}$ and $\mathbf{G}$ are the vectors of the fluxes in the curvilinear coordinates. These vectors can be expressed in terms of the corresponding vectors in Cartesian coordinates $\mathbf{Q}_c$, $\mathbf{E}_c$, and $\mathbf{G}_c$:

$$\mathbf{Q} = J\mathbf{Q}_c, \quad \mathbf{E} = J\left(\mathbf{E}_c \frac{\partial \xi}{\partial x} + \mathbf{G}_c \frac{\partial \xi}{\partial y}\right), \quad \mathbf{G} = J\left(\mathbf{E}_c \frac{\partial \eta}{\partial x} + \mathbf{G}_c \frac{\partial \eta}{\partial y}\right)$$

where $J = \det \|\partial(x, y)/\partial(\xi, \eta)\|$ is the Jacobian of the transformation. The vector components in Cartesian coordinates for the 2D Navier-Stokes equations are:

$$\mathbf{Q}_c = \begin{bmatrix} \rho \\ \rho u \\ \rho v \\ e \end{bmatrix}, \qquad \mathbf{E}_c = \begin{bmatrix} \rho u \\ \rho u^2 + p - \dfrac{1}{\mathrm{Re}_\infty}\tau_{xx} \\ \rho uv - \dfrac{1}{\mathrm{Re}_\infty}\tau_{xy} \\ \rho uH - \dfrac{1}{\mathrm{Re}_\infty}\left(u\tau_{xx} + v\tau_{xy} + \dfrac{\mu}{\mathrm{Pr}(\gamma-1)\mathrm{M}_\infty^2}\dfrac{\partial T}{\partial x}\right) \end{bmatrix},$$

$$\mathbf{G}_c = \begin{bmatrix} \rho v \\ \rho uv - \dfrac{1}{\mathrm{Re}_\infty}\tau_{xy} \\ \rho v^2 + p - \dfrac{1}{\mathrm{Re}_\infty}\tau_{yy} \\ \rho vH - \dfrac{1}{\mathrm{Re}_\infty}\left(u\tau_{xy} + v\tau_{yy} + \dfrac{\mu}{\mathrm{Pr}(\gamma-1)\mathrm{M}_\infty^2}\dfrac{\partial T}{\partial y}\right) \end{bmatrix}$$

Here, ρ is the density, u and v are the components of the velocity vector $\mathbf{V}$, p is the pressure, T is the temperature, e is the total energy per unit volume, H is the specific enthalpy, $\boldsymbol{\tau}$ is the stress tensor with the components

$$\tau_{xx} = \mu\left(-\frac{2}{3}\mathrm{div}\,\mathbf{V} + 2\frac{\partial u}{\partial x}\right), \quad \tau_{xy} = \mu\left(\frac{\partial u}{\partial y} + \frac{\partial v}{\partial x}\right), \quad \tau_{yy} = \mu\left(-\frac{2}{3}\mathrm{div}\,\mathbf{V} + 2\frac{\partial v}{\partial y}\right),$$

and μ is the dynamic viscosity calculated from the power law $\mu = T^{0.7}$.

The system of equations is closed by the equation of state of a perfect gas $p = \rho T/(\gamma \mathrm{M}_\infty^2)$. The Navier-Stokes equations are written in nondimensional form. The dependent variables are scaled to the corresponding free-stream parameters and the pressure to twice the pressure head. The coordinates are scaled to the

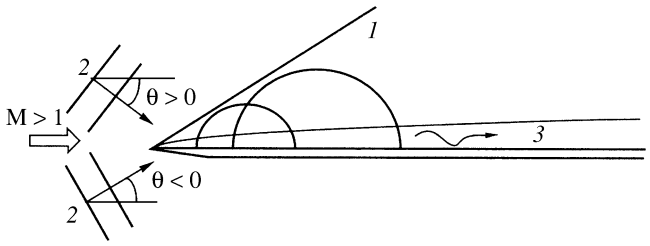

Fig. 2. Scheme of the receptivity of a supersonic boundary layer to acoustic disturbances: *1* — shock wave, *2* — acoustic waves, *3* — boundary layer

characteristic length L and time to the ratio of L and the free-stream velocity, Re_∞ is the Reynolds number, γ is the specific heat ratio, and Pr is the Prandtl number. In this study, it is assumed that $\gamma = 1.4$ and $\mathrm{Pr} = 0.72$.

The problem was solved numerically using an implicit finite-volume method of the second order with respect to space and time. A quasi-monotonous scheme of the Godunov type was used. This is very important for problems in which the calculation domain contains shock waves. In [11], a steady-state solution of the problem of the flow over a flat plate with a sharp leading edge was obtained and it was shown that this scheme can be used for problems of the stability of the boundary layer on a plate.

In this study, we will numerically model the receptivity to acoustic disturbances. The calculation domain is rectangular, with a base that coincides with the plate surface. On this boundary, the no-slip conditions, i.e. zero velocity components, are specified. The plate surface is adiabatic: $\partial T_w/\partial n = 0$. On the right boundary, linear extrapolation of the dependent variables u, v, p, and T is used.

The calculation domain containing 1501×201 grid points is condensed in the boundary layer region near the body surface and near the leading edge of the plate, where a shock wave is formed. The problem is solved in two stages. First, a numerical solution is found for a longitudinal flow over the flat plate at $\mathrm{M}_\infty = 6$ and $\mathrm{Re}_\infty = 2 \cdot 10^6$, where the Reynolds number is based on the plate length L. On the left and top boundaries, free-stream conditions are specified. The pressure field calculated for steady-state flow over the plate is shown in Fig. 1. The visco-inviscid interaction results in the formation of a shock wave attached to the leading edge of the plate. As shown below, this shock plays an important role in the receptivity process near the leading edge. In the second stage, after calculating the steady-state solution for the flow over the flat plate, a plane monochromatic acoustic wave was added to the free stream (Fig. 2) by means of perturbations of the dependent variables:

$$(u',\ v',\ p',\ T')_\infty^{\mathrm{T}} = (|u'|,\ |v'|,\ |p'|,\ |T'|)_\infty^{\mathrm{T}} \exp[i(k_x x + k_y y - \omega t)]$$

where, $|u'|$, $|v'|$, $|p'|$, $|T'|$ are the nondimensional perturbation amplitudes related by the formulas

$$\begin{gathered} |p'| = \varepsilon, \qquad |u'| = \pm \mathrm{M}_\infty |p'| \cos\theta, \\ |v'| = \mp \mathrm{M}_\infty |p'| \sin\theta, \qquad |T'| = (\gamma - 1)\mathrm{M}_\infty^2 |p'| \end{gathered} \tag{1.1}$$

where, θ is the angle of incidence of the acoustic wave. This angle is positive (negative) when the acoustic wave is above (below) the plate, ε is a small parameter characterizing the wave amplitude, $k_x = k_\infty \cos\theta$, $k_y = -k_\infty \sin\theta$ are the wave vector components, ω is the nondimensional frequency, and $k_\infty = \omega/(\cos\theta \pm 1/\mathrm{M}_\infty)$. In formulas (1.1), the upper (lower) sign corresponds to the fast (slow) acoustic wave. If $\theta = 0^\circ$, then

$$\begin{gathered} k_x = k_\infty, \qquad k_y = 0, \qquad |u'| = \pm \mathrm{M}_\infty |p'|, \\ |v'| = 0, \qquad |p'| = \varepsilon, \qquad |T'| = (\gamma - 1)\mathrm{M}_\infty^2 |p'| \end{gathered}$$

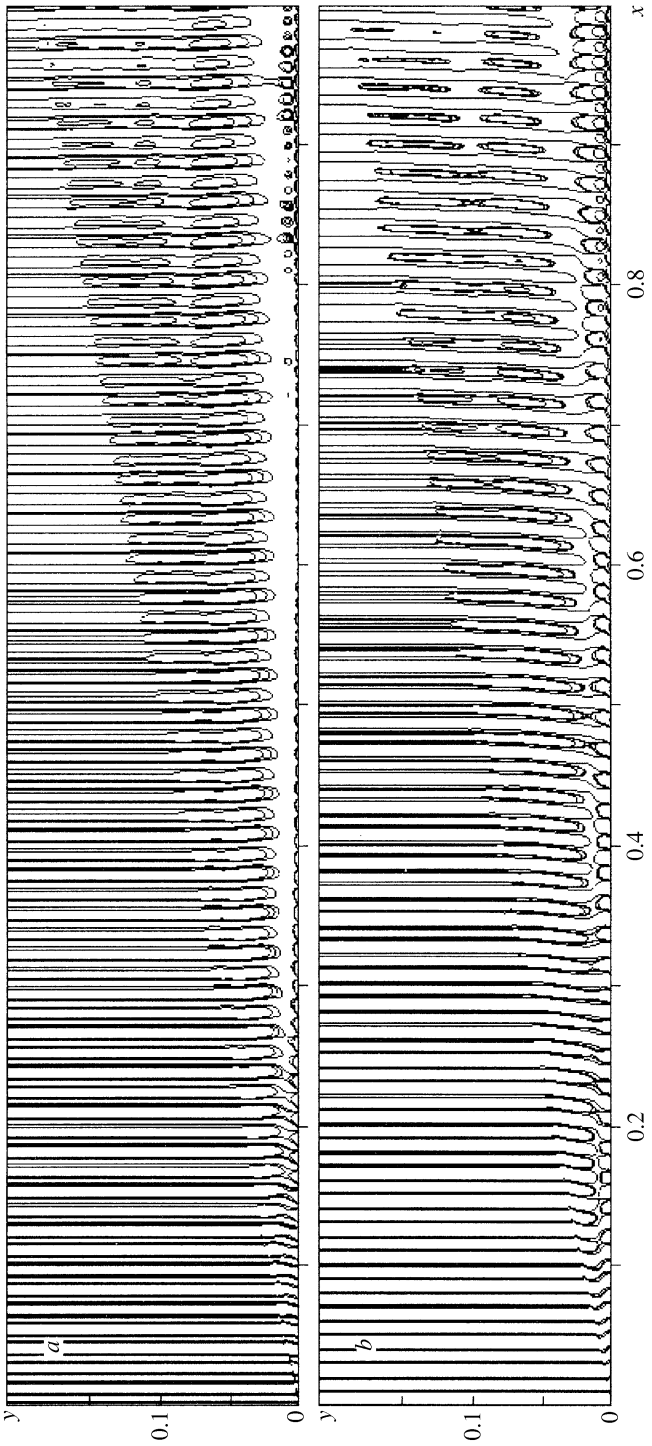

Fig. 3. Pressure perturbation fields induced by the fast (*a*) and slow (*b*) acoustic waves for $\theta = 0^\circ$

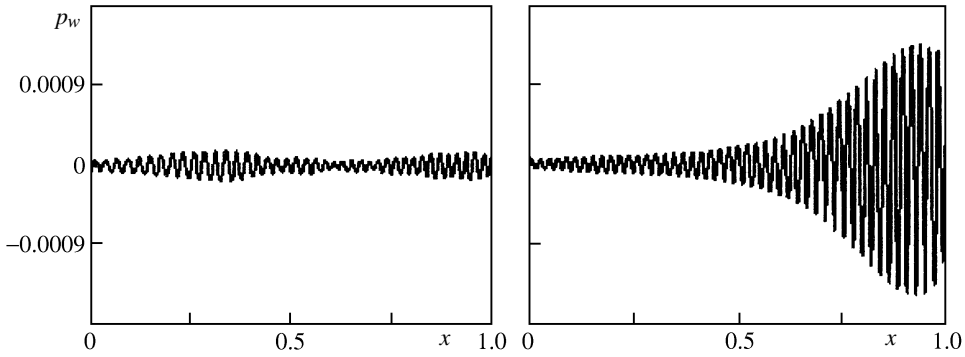

Fig. 4. Pressure perturbations on the plate surface, induced by the fast (*a*) and slow (*b*) acoustic waves for $\theta = 0^\circ$

For positive angles θ (the wave impinges from above), perturbations (1.1) were added on the left and upper boundaries of the calculation domain. For negative θ (the wave impinges from below), the perturbations were introduced on the left boundary of the calculation domain, while on the upper boundary the "soft" boundary conditions were specified. On the plate surface, the temperature perturbations were zero ($T'(y = 0) = 0$), i.e. in solving the unsteady problem the wall temperature was equal to the adiabatic-wall temperature obtained from the solution of the steady-state problem: $T_w(x, t) = T_{ad}(x)$.

To model the receptivity of the boundary layer with respect to acoustic disturbances, a fast (or a slow) acoustic wave was introduced into the free stream after calculating the steady-state flow field. The amplitude of these waves was small ($\varepsilon = 5 \cdot 10^{-5}$). This ensured the linearity of the receptivity process. The nondimensional frequency was $\omega = 260$, which corresponded to a frequency parameter $F = \omega/\mathrm{Re} = 1.3 \cdot 10^{-4}$. We note that the perturbation amplitude should be much greater than the calculation error in the solution of the steady problem. For small amplitudes of the acoustic waves, this solution, obtained with high accuracy, results in a significant increase in the unperturbed flow field calculation time. The Navier-Stokes equations were integrated up to the instant of attainment of the steady-state periodic regime.

2. ACOUSTIC WAVES WITH ZERO ANGLE OF INCIDENCE

First, we performed a numerical simulation for zero angle of incidence of the acoustic wave ($\theta = 0^\circ$). The difference between the solutions of the unsteady and steady problems at a given instant of time gives the instantaneous disturbance field. A typical pattern of the pressure disturbances induced by the fast and slow acoustic waves is shown in Figs. 3*a* and *b*. Clearly, the shock wave perturbs the acoustic field only slightly.

Let us consider the case of a fast incident acoustic wave. After entering the boundary layer, the acoustic wave is synchronized with the fast mode in the boundary layer (F-mode in the terminology of [8]). This results in a monotonous increase in the amplitude of the F-mode on the interval $0 < x < 0.2$ (see the one-cell structures in the boundary layer). Downstream, the phase velocity of the F-mode decreases, desyncronization occurs, the disturbances decrease, and the F-mode is damped. Then, the F-mode is synchronized with an unstable slow mode in the boundary layer (S-mode in the terminology of [8] or the second mode in Mack's terminology [12]) and excites the latter via the inter-mode exchange mechanism (see [7]), $0.6 < x < 0.7$. Downstream, the S-mode grows due to the instability, which results in the formation of two-cell structures in the boundary layer, $0.8 < x < 1$ (see Fig. 3*a*). These phenomena are clearly visible in the surface distribution of the pressure disturbance on the plate (Fig. 4*a*). The above scenario agrees with that described by asymptotic theory [6–8] and the numerical simulation results [5].

Figure 5 shows the instantaneous field of the density disturbances induced by the fast acoustic wave. In the critical layer, where the mean velocity is close to the phase velocity and the density disturbances are maximum, the disturbances form a trail of cells. In the region $x < 0.7$, the neighboring cells are separated, which is typical of the F-mode. Downstream, the neighboring cells start to overlap and form a spindle-

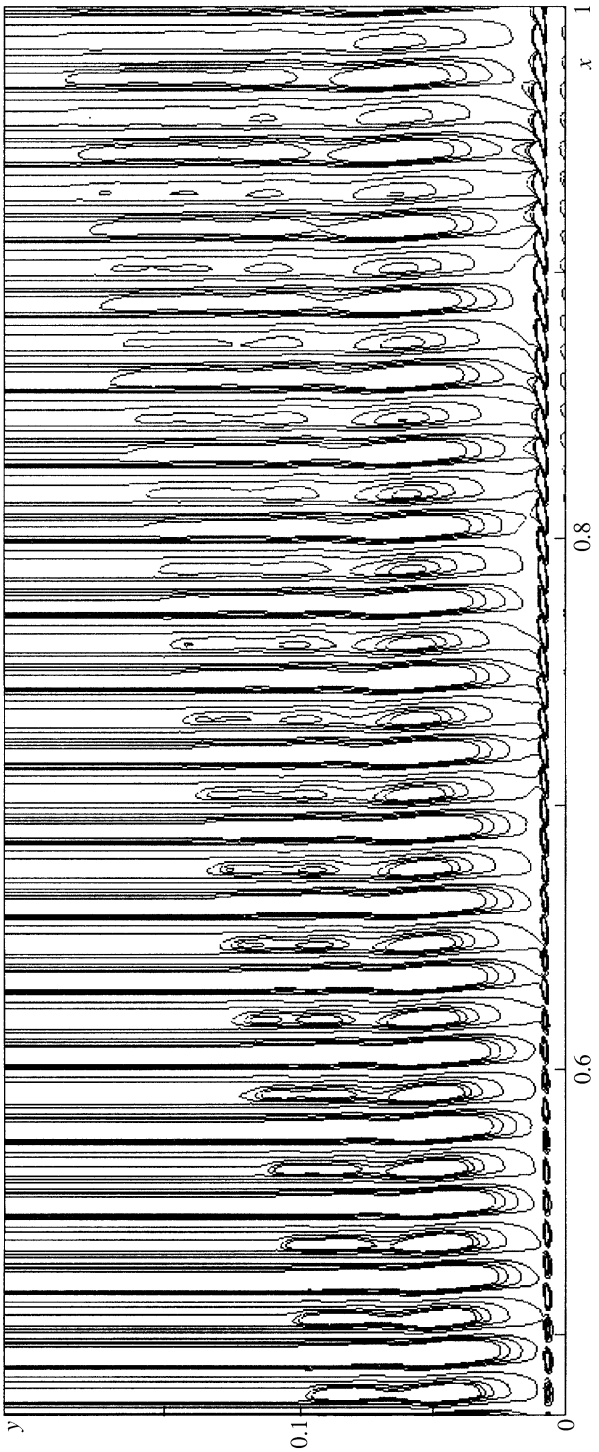

Fig. 5. Density perturbations induced by the fast acoustic wave for $\theta = 0^\circ$

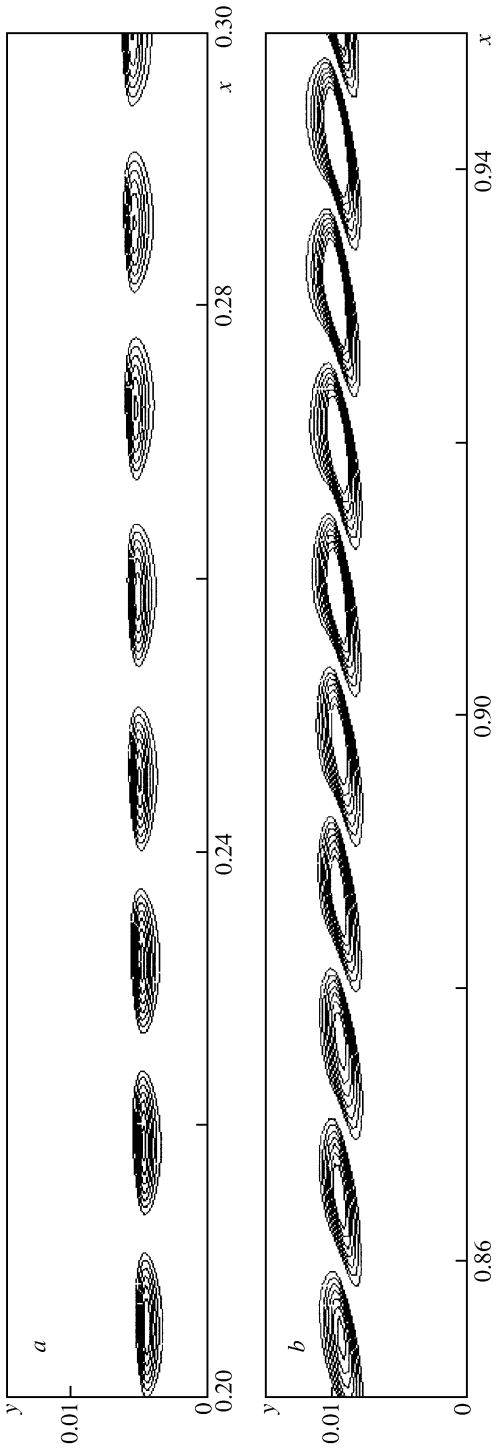

Fig. 6. Density perturbations induced by the fast acoustic wave: *a* — *F*- mode, *b* — *S*-mode

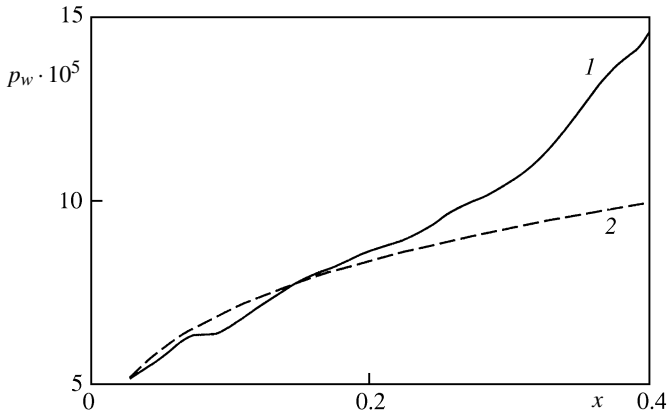

Fig. 7. Pressure perturbation amplitude on the wall near the leading edge of the plate: *1* — numerical modeling, *2* — asymptotic theory [6–8]

shaped structure ($0.8 < x < 1$), which is typical of the *S*-mode. A detailed fragment of these structures is shown in Fig. 6*a* for the *F*-mode ($0.2 \le x \le 0.3$) and in Fig. 6*b* for the *S*-mode ($0.85 \le x \le 0.95$). We also note that the pattern of the pressure disturbances induced by the fast acoustic wave coincides qualitatively with the numerical simulation results [5].

In contrast to the case of a fast acoustic wave, according to theoretical studies [6–8], near the leading edge the slow acoustic wave is directly synchronized with the *S*-mode. This results in an algebraic (of the order of $x^{1/4}$) growth in the *S*-mode amplitude starting from the plate tip [6–8]. Figure 7 shows that the theoretical dependence corresponds fairly well to the disturbance growth near the leading edge obtained by direct numerical simulation. Downstream, the *S*-mode becomes unstable and its amplitude increases exponentially. At $x \approx 0.9$, the maximum amplitude of the *S*-mode is much greater than the maximum amplitude induced by the fast acoustic wave. This is clear from Fig. 4*b* which shows the pressure disturbance on the plate surface as a function of the x coordinate at a fixed instant of time. Such behavior is consistent with theoretical studies [6–8]. In the case of a slow incident acoustic wave, a spindle-shaped pressure disturbance structure (similar to that in Fig. 6*b*) is formed in the critical layer directly adjacent to the leading edge, which once again indicates the predominance of the *S*-mode in this region.

This interesting feature is observed outside the boundary layer for both fast and slow incident acoustic waves. Just above the boundary layer, the pressure disturbance amplitude is relatively small (Fig. 3). A "silence" zone separates the disturbances in the boundary layer and the outer acoustic field. This zone expands downstream, which agrees with the theoretical solution [6–8] for acoustic disturbances in the diffraction zone.

3. ACOUSTIC WAVES WITH DIFFERENT ANGLES OF INCIDENCE

The results of numerical modeling for fast and slow acoustic waves with angles of incidence $\theta = +45^\circ$ (from above) and -45° (from below) reveal new features of the receptivity not described by the asymptotic theory [6–8]. These phenomena are related with the interaction of the incident acoustic wave with the shock wave near the leading edge of the plate. It is known that in passing through the shock the acoustic wave changes amplitude and forms entropy and vorticity waves behind the shock [13]. In addition, the acoustic waves enter the boundary layer and are reflected back from the plate surface. These effects may change the disturbance field between the plate surface and the shock, particularly near the leading edge of the plate, where the visco-inviscid interaction is maximum.

The pressure disturbance distributions over the plate surface are shown in Fig. 8 for different cases. The left column corresponds to the incidence of a fast acoustic wave and the right column to a slow wave with incidence angles $\theta = +45^\circ$ (upper row) and -45° (lower row). Clearly, in all cases the slow acoustic wave generates stronger disturbances downstream than the fast wave. However, in a supersonic boundary layer

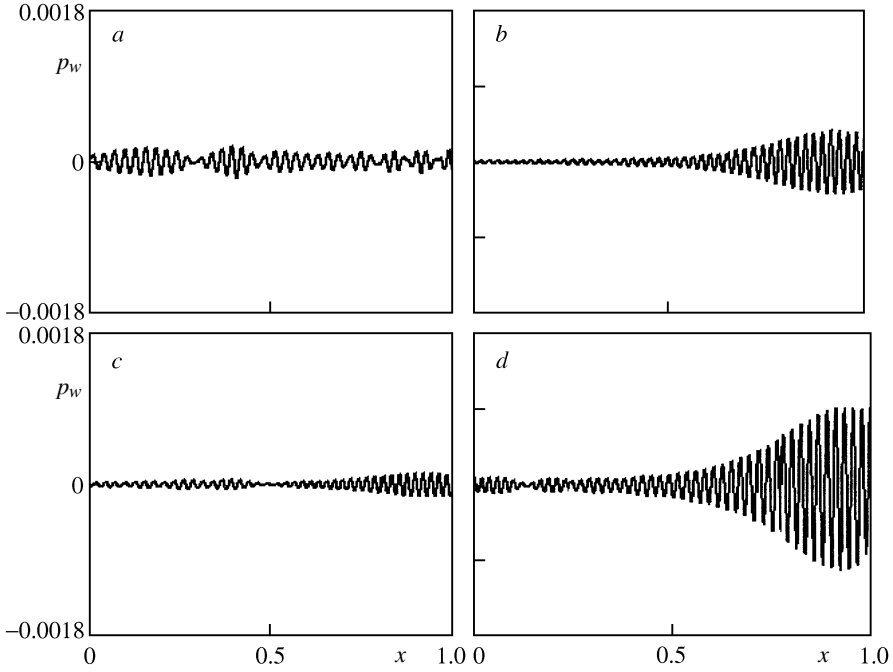

Fig. 8. Pressure perturbation distributions over the plate surface, induced by the fast and slow acoustic waves for incidence angles $\theta = +45^\circ$ (*a*, *b*) and $\theta = -45^\circ$ (*c*, *d*)

the growth of an unstable mode also depends on the incidence angle (Fig. 8*b*, *d*). A slow acoustic wave with an incidence angle $\theta = +45^\circ$ (incidence from above) generates weaker disturbances than a wave with $\theta = -45^\circ$ (incidence from below). To understand the reasons for this behavior, it is necessary to consider the phenomena occurring near the leading edge of the plate.

The pressure disturbance field ($0 \le x \le 0.15$) for a slow acoustic wave with incidence angles $\theta = +45^\circ$ (Fig. 9*a*) and -45° (Fig. 9*b*) reveals that the shock and the plate surface form a wedge-shaped wave guide in which the disturbances propagate downstream. The outer disturbances penetrate the shock and generate forced acoustic oscillations. The forced disturbances have two components: the first is related with the penetration of the acoustics through the shock and the second is related with the scattering of the acoustic waves by the plate tip. The slow acoustic wave with an angle of incidence $\theta = +45^\circ$ barely penetrates the shock and the wave guide is not excited (Fig. 9*a*). On the contrary, the wave with $\theta = -45^\circ$ is amplified on passing through the shock and generates oscillations in the wave guide (Fig. 9*b*). The numerical results agree qualitatively with the linear theory of acoustic-wave passage through an oblique shock [13]. In particular, in accordance with the linear theory [13] the coefficient of transmission of the slow acoustic wave with $\theta = +45^\circ$ through the shock considered is zero. This acoustic wave does not penetrate the shock, as also obtained in the numerical modeling. For the slow acoustic wave with $\theta = -45^\circ$, the transmission coefficient is greater than unity, i.e. the wave is amplified, which agrees with the calculation results. We note that the linear theory does not take into account the reflections of the acoustic wave from the plate surface or the nonuniformity of the mean flow field. Thus, the interaction of the acoustic waves with the shock near the leading edge of the plate may play an important role in the receptivity of the supersonic boundary layer.

A similar situation was observed for other angles of incidence of the fast or slow acoustic wave. Thus, a fast acoustic wave with $\theta = +45^\circ$ is amplified on passing through the shock, while a wave with $\theta = -45^\circ$ fails to penetrate the shock. The pressure disturbance amplitudes on the wall for these cases are compared in Fig. 8*a*, *c*.

The linear theory [13] also makes it possible to determine the amplitudes of the entropy and vorticity waves formed after the passage of the acoustic wave through an oblique shock. Our numerical simulation shows that the amplitudes of these disturbances are small in all the cases considered.

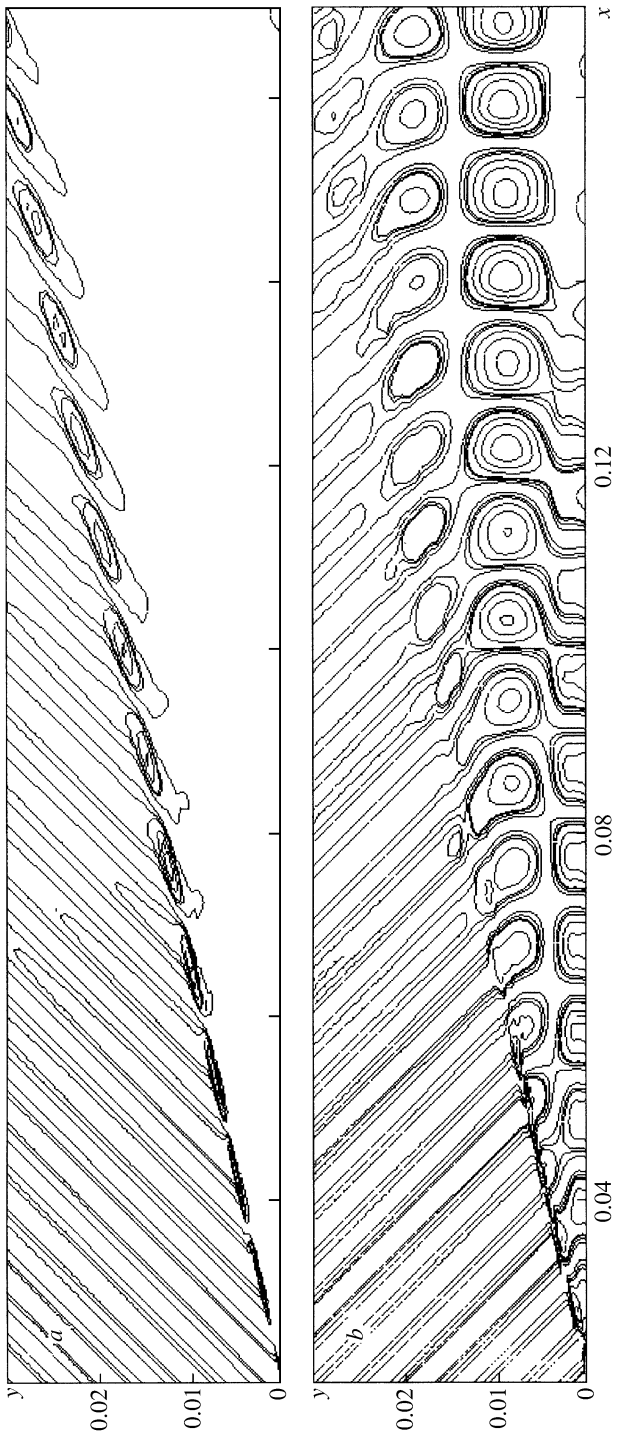

Fig. 9. Pressure perturbation field ($0 \le x \le 0.15$) in the case of a slow acoustic wave incident at angles $\theta = +45^\circ$ (*a*) and $\theta = -45^\circ$ (*b*)

Thus, when an acoustic wave impinges at a finite angle to the leading edge of the plate, two factors affecting the growth of the unstable mode in the boundary layer are manifested. The first is associated with the phase difference between the incident acoustic waves and the unstable boundary layer mode (*S*-mode.) The second factor is associated with the passage of the acoustic waves through the shock and the excitation of a wedge-shaped wave guide.

Summary. The receptivity of a supersonic boundary layer on a flat plate with a sharp leading edge with respect to acoustic disturbances is simulated numerically. The propagation of disturbances in the boundary layer induced by fast and slow acoustic waves incident on the plate from above and from below is investigated. It is shown that the shock formed near the leading edge due to the visco-inviscid interaction may significantly affect the acoustic field and the receptivity process. This effect is not taken into account in the linear theory.

The results for fast and slow acoustic waves incident on the leading edge at zero angle are in qualitative agreement with the results of theoretical studies and calculations.

Near the leading edge, the shock and the plate surface form a wedge-shaped wave guide in which the acoustic modes propagate downstream. The disturbance field in this wave guide depends on the type and incidence angle of the acoustic wave. A slow acoustic wave with an incidence angle $\theta = +45^\circ$ (from above) and a fast wave with $\theta = -45^\circ$ (from below) are characterized by weak shock penetration, and the wave guide is not excited. On the contrary, a slow acoustic wave with $\theta = -45^\circ$ and a fast wave with $\theta = +45^\circ$ are amplified on passing through an oblique shock and efficiently excite oscillations in the wave guide. The level of the acoustic near-field plays an appreciable role in the receptivity processes and the downstream development of the disturbances. These numerical examples show that even a weak shock can significantly affect the disturbance field near the leading edge and the receptivity process.

In addition, the development of the unstable boundary layer mode depends on the difference in phase between this mode and the acoustic disturbances. An increase in the phase shift results in a reduction in the unstable-mode amplitude. The action of these two factors (desynchronization and the excitation of the wave guide) results in a nonmonotonous dependence of the receptivity rate on the angle of incidence of the acoustic wave. Moreover, when the slow acoustic wave impinges from below the downstream disturbances are greater than when the wave impinges from above. This calls for further theoretical, numerical, and experimental investigation.

REFERENCES

1. H. L. Reed, R. Kimmel, S. Schneider, and D. Arnal, "Drag prediction and transition in hypersonic flow," *AIAA Paper*, No. 97–1818 (1997).
2. S. A. Gaponov and A. A. Maslov, *Disturbance Development in Compressible Flows* [in Russian], Nauka, Novosibirsk (1980).
3. X. Zhong, "Leading-edge receptivity to free-stream disturbance waves in hypersonic flow over parabola" *J. Fluid Mech.*, **441**, 315–367 (2001).
4. Y. Ma and X. Zhong, "Receptivity of a supersonic boundary layer over a flat plate. Pt 1. Wave structures and interactions", *J. Fluid Mech.*, **488**, 31–78 (2003).
5. Y. Ma and X. Zhong, "Receptivity of a supersonic boundary layer over a flat plate. Pt 1. Receptivity to free-stream sound", *J. Fluid Mech.*, **488**, 79–121 (2003).
6. A. V. Fedorov and A. P. Khokhlov, "Excitation of unstable modes in a supersonic boundary layer by acoustic waves," *Fluid Dynamics*, **26** No. 4, 531–537 (1991).
7. A. V. Fedorov and A. P. Khokhlov, "Prehistory of instability in a hypersonic boundary layer," *Theoret. Comput. Fluid Dyn.*, **14**, No. 6, 359–375 (2001).
8. A. V. Fedorov, "Receptivity of high-speed boundary layer to acoustic disturbances," *J. Fluid Mech.*, **491**, 101–129 (2003).
9. A. A. Maslov and N. V. Semenov, "Excitation of natural oscillations in a boundary layer by an external acoustic field," *Fluid Dynamics* **21**, No. 3, 400–403 (1986).

10. A. A. Maslov, A. N. Shiplyuk, A. Sidorenko, and D. Arnal, "Leading-edge receptivity of a hypersonic boundary layer on a flat plate," *J. Fluid Mech.*, **426**, 73–94 (2001).
11. I. V. Egorov, V. G. Sudakov, and A. V. Fedorov, "Numerical modeling of perturbation propagation in a supersonic boundary layer," *Fluid Dynamics*, **39**, No. 6, 874–884 (2004).
12. L. M. Mack, "Linear stability theory and the problem of supersonic boundary layer transition," *AIAA J.*, **13**, No. 3, 278–289 (1975).
13. S. P. Dyakov, "Interaction of shock waves with small disturbances. 1," *Zh. Exp. Tekh. Fiz.*, **33**, No. 4(10), 948–961 (1957).